Natural Resources for Human Health

eISSN: 2583-1194

Original Research

Received 14 July 2026
Revised 15 Aug 2026
Accepted 02 Sep 2026

Natural Resources for Human Health 2026, Vol. 6 (20s): 497–516

KEYWORDS:
Air quality prediction, Canonical correlation analysis, Carbon monoxide, Heavy fuel oil, IPCC Tier 1 inventory, Sulphur dioxide.

Linking Fuel-based Greenhouse Gas Emissions with Ambient Combustion Pollutants in a Brick Kiln Cluster: A Principal Component Regression Framework for Baghdad, Iraq

Sarah Duraid Ahmed Zangana[1,2], Noor Faizah Fitri, Md Yusof[1,*]

[1]School of Civil Engineering, Universiti Sains Malaysia, Penang, Malaysia.
[2]Ministry of Environment, Baghdad, Iraq
*Corresponding Author Email: noorfaizah@usm.my
ORCID: 0000-0002-7939-4318

ABSTRACT: Traditional brick kilns burning high-sulphur heavy fuel oil contribute to air pollution and greenhouse gas emissions in Iraq, but integrated assessments remain limited. This study quantified ambient pollutants in Al-Nahrawan, Baghdad, and modelled their associations with meteorology and fuel-based emissions. Sulphur dioxide (SO_2), nitrogen dioxide (NO_2), volatile organic compounds (VOCs) and carbon monoxide (CO) were measured at 21 sites across four seasons in 2024, yielding 672 observations. Carbon dioxide (CO_2), methane and nitrous oxide emissions were estimated using the IPCC 2006 Tier 1 method and combined as CO_2-equivalent (CO_2-eq). Spearman correlation and canonical correlation analysis assessed associations among pollutants, temperature, wind speed and CO_2-eq. Pollutant-specific principal component regression models excluded each target pollutant from its predictor set and underwent 10-fold cross-validation. Estimated emissions ranged from 9.36 to 14.48 Gg CO_2 per factory, proportional to fuel consumption. Maximum site-level seasonal means occurred in summer: 0.48 ppm for SO_2 and NO_2 and 61.25 ppm for CO, with frequent exceedances of Iraqi limits and WHO guidelines. The first canonical correlation was 0.878 (Wilks' $\Lambda = 0.220$; $p < 0.001$), dominated by temperature. Two components representing combustion–thermal intensity and wind dispersion explained approximately 75% of predictor variance. Models explained 69.5–77.6% of pollutant variability, with mean cross-validated R^2 values of 0.680–0.859. This low-cost screening framework supports fuel sulphur limits, improved combustion control and intensified summer monitoring to identify high-risk periods. Independent validation is required before application elsewhere.

1. INTRODUCTION

Fossil-fuel combustion is the dominant driver of anthropogenic climate change and a major source of ambient air pollution (Chien et al, 2023; IPCC, 2021). Besides carbon dioxide (CO_2), combustion releases methane (CH_4), nitrous oxide (N_2O), carbon monoxide (CO) and non-methane volatile organic compounds (NMVOCs), while most of the sulphur contained in the fuel is emitted as sulphur dioxide (SO_2) (Amous, 2000). Nitrogen dioxide (NO_2), SO_2 and CO are regulated as criteria air pollutants because of their well-documented effects on respiratory and cardiovascular health (WHO,2021; EPA, 2024). Because air pollutants and greenhouse gases (GHGs) share the same combustion sources, measures that reduce one group frequently reduce the other, which makes their joint assessment relevant to both air-quality management and climate policy (Afifa et al, 2024).

The buildings and construction sector accounts for about 37% of global energy- and process-related CO_2 emissions (UNEP, 2024), and fired-clay brick production is one of its most energy- and pollution-intensive upstream activities (Labaran et al, 2021; Valdes et al ,2020). Traditional kilns operate with poor control of combustion air and temperature and frequently burn low-grade fuels, so they emit large quantities of SO_2, nitrogen oxides (NO_x), CO, VOCs, particulate matter and GHGs relative to their output (Valdes et al, 2020; Seay et al,2021; Gomes & Hossain,2003; Ukwatta et al, 2018). Most field evidence comes from coal- and biomass-fired kilns in South Asia (Seay et al,2021; Haque et al,2022; Weyant et al, 2016), whereas kilns fired with residual heavy fuel oil, which are common in the Middle East, have received much less attention. In Iraq, the Al-Nahrawan area east of Baghdad hosts more than 170 closely spaced brick factories that burn high-sulphur heavy fuel oil near residential and agricultural land (Ministry of Environment,2024). Earlier studies in this area reported exceedances of Iraqi standards for SO_2, NO_2 and VOCs (Al Nuzal et al, 2018) and deteriorating air quality detectable in satellite observations (Jadem et al, 2023); however, these studies were descriptive and did not link ambient concentrations with fuel consumption or GHG emissions.

Two methodological traditions are commonly used to assess such sources. Emission inventories based on the Intergovernmental Panel on Climate Change (IPCC) guidelines estimate GHG emissions from fuel-consumption activity data and emission factors and are widely applied where facility-level measurements are lacking (Amous, 2000; IPCC, 2006). Air-quality studies, by contrast, model measured concentrations using linear regression (Hu et al, 2024; Kazi et al, 2023; Moradi et al, 2024), artificial neural networks and other machine-learning methods (Hosamane & Desai, 2018; Pasic et al,2020; Shatnawi & Abu-Qdais,2021; Ge et al, 2021; Castelli et al, 2020; Rawat et al, 2026; Lawrence & Bhathmanabhan, 2026,), or multivariate statistical techniques. Among the latter, principal component analysis (PCA), principal component regression (PCR) and canonical correlation analysis (CCA) have been used to relate pollutant concentrations to meteorological variables while handling the strong collinearity typical of environmental data (Pasic et al, 2023; Shihab, 2022; Song et al, 2020; Statheropoulos et al, 1998). More recently, forecasting systems have begun to combine emission, meteorological and pollutant information within a single model (Geng et al, 2026).

Nevertheless, these two traditions are rarely combined at the scale of an industrial cluster. Inventory studies seldom compare their estimates with measured ambient concentrations, and statistical air-quality models usually rely on meteorology alone as the explanatory variable set (Shihab, 2022; Song et al, 2020; Statheropoulos et al, 1998). To the best of our knowledge, no study has linked IPCC-based GHG estimates with multi-season ambient measurements of SO_2, NO_2, VOCs and CO in a brick kiln cluster fired with heavy fuel oil or used this combined information to estimate ambient pollutant concentrations.

This study addresses that gap in the Al-Nahrawan brick kiln cluster. Its objectives were to: (i) estimate CO_2, CH_4 and N_2O emissions from kiln fuel consumption using the IPCC 2006 Tier 1 method; (ii) characterize the spatial and seasonal variation of ambient SO_2, NO_2, VOCs and CO at 21 sites and compare it with Iraqi and World Health Organization (WHO) limits; (iii) quantify the pairwise and multivariate associations among pollutants, temperature, wind speed and CO_2-equivalent (CO_2-eq) using Spearman correlation and CCA; and (iv) develop and cross-validate pollutant-specific PCA–PCR models for estimating ambient concentrations. It was hypothesized that ambient pollutant levels co-vary with fuel-based emission intensity and thermal conditions and are modulated by wind dispersion. The resulting framework is intended as a screening tool to support targeted monitoring and regulation in brick kiln clusters.

2. MATERIALS AND METHODS

2.1 Study Area and Data Set

The Al-Nahrawan Industrial Area in Baghdad, Iraq, was selected as the study area because it contains a high concentration of brick manufacturing facilities in proximity to residential areas. This area contains over 170 closely spaced brick factories that utilize traditional kilns and residual heavy fuel oil (black oil) (Ministry of Environment, 2024). These facilities rely on inefficient side or roof combustion systems, requiring high temperatures, which results in incomplete combustion. Consequently, they emit high concentrations of air pollutants, posing significant environmental and health risks to the surrounding population. Figure1 shows the geographical location of the Al-Nahrawan Industrial Area in Baghdad, Iraq.

Natural Resources for Human Health
eISSN: 2583-1194

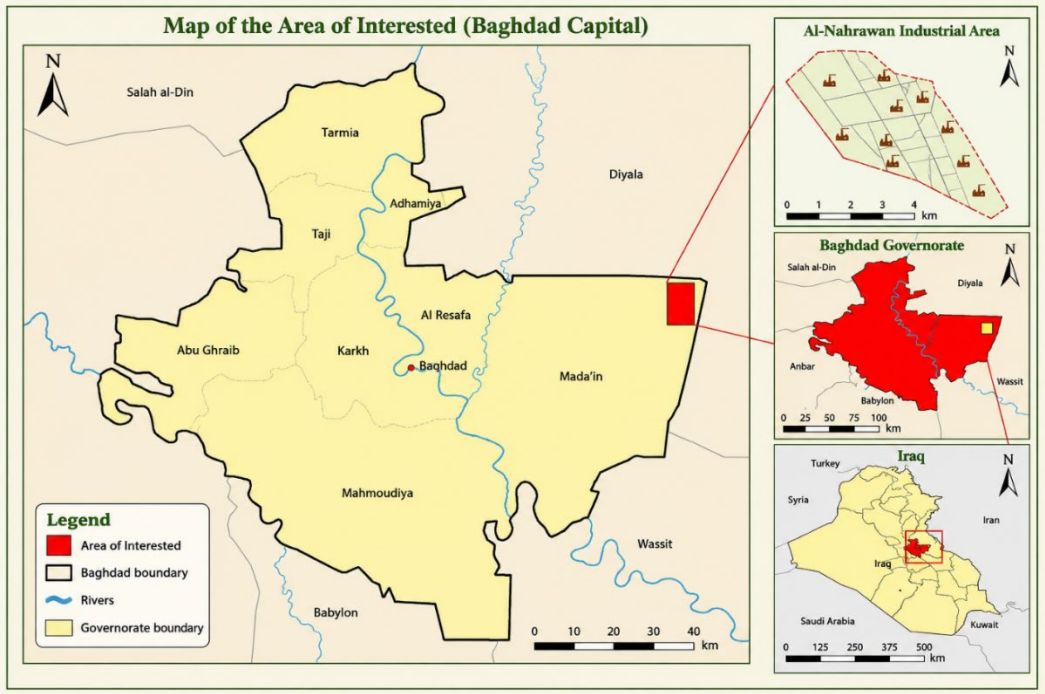


Figure 1: Geographical Location of the Study Area in the Al-Nahrawan Region, Baghdad Governorate, Iraq

The data was collected from the industrial area (brick factory complex). The study evaluated greenhouse gas emissions from Iraq's brick industry by utilizing IPCC methodologies, specifically focusing on data collected from the industrial area of brick factories. The research employed the Tier 1 methodology as outlined in the IPCC 2006 guidelines, which relies on default emission factors based on fuel type, specifically fuel oil as shown in Figure 2 (IPCC, 2006; Minx et al, 2017; Yousefi et al, 2016). Although higher-tier methodologies may provide greater estimation accuracy through the use of site-specific emission factors and detailed operational data, such information was not available for the investigated facilities. Therefore, the Tier 1 approach was considered the most appropriate and transparent methodology for the objectives of this study. The use of default emission factors introduces a degree of uncertainty because they represent generalized combustion conditions rather than site-specific characteristics. Nevertheless, the Tier 1 methodology is widely accepted for preliminary emission inventories and regional environmental assessments, providing a consistent basis for comparative analyses and environmental decision-making.

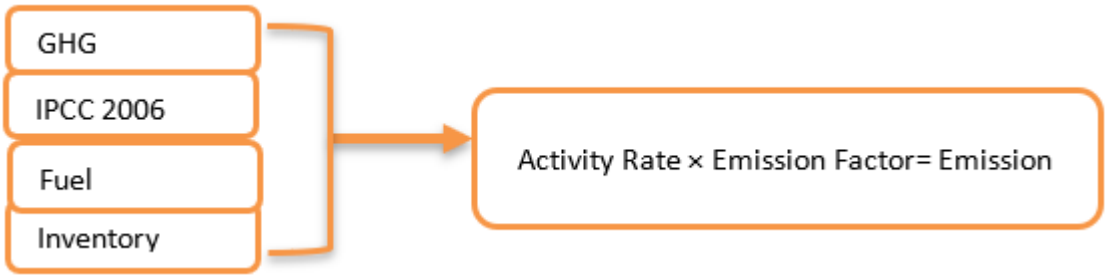


Figure 2: The Workflow of the Emission Inventory Software Using IPCC

Ambient air pollutants (SO_2, NO_2, VOCs, and CO) were measured at 21 strategically selected monitoring sites within the study area, as shown in Figure 3. Measurements were conducted during four seasons, with eight repeated measurements obtained at each monitoring site during each season. Accordingly, the complete dataset comprised 672 observations (21 monitoring sites × 4 seasons × 8 repeated measurements). Meteorological data, including ambient temperature and wind speed, were obtained from Weather Spark, while GHG emissions were estimated using the IPCC Tier 1 methodology based on the corresponding fuel-consumption data. The resulting dataset was compiled for subsequent multivariate statistical analyses and predictive modelling. The sampling sites were distributed across the study area to ensure representative spatial coverage of the major brick

manufacturing activities and potential emission hotspots. The final statistical data set was at the level of repeated readings when applicable. Field measurements were taken under similar operating conditions and during the same daily monitoring window to minimize short-term temporal bias, and kiln activity. The air pollutants were measured using a portable HAZ-Scanner HIM-6000 multigas monitor (Environmental Devices Corporation, USA). Quality assurance and quality control procedures were implemented throughout the monitoring campaign to ensure data reliability. Before each field survey, the HAZ-Scanner HIM-6000 was inspected and calibrated according to the manufacturer's operating instructions. Instrument performance was verified through routine zero checks and operational self-diagnostic functions before each sampling session. All measurements were conducted under consistent operating conditions using the same instrument and standardized sampling procedures. To improve measurement reliability, repeated readings were obtained at each monitoring location, and abnormal observations were carefully examined and excluded only when instrumental or operational errors were identified. Field records were reviewed immediately after each monitoring campaign to verify data completeness and consistency prior to statistical analysis.

Measurements were conducted over a year (2024) across four seasons: winter (January), spring (March), summer (June), and fall (September). All pollutant concentrations were reported in parts per million (ppm). Where air quality standards were originally expressed in milligrams per cubic meter (mg/m^3), values were converted to ppm under standard temperature and pressure conditions to ensure consistency. Baseline meteorological conditions, specifically ambient air temperatures (T, °C) and wind speeds (W, mi/hr), were obtained from Weather Spark (Weather Spark, 2024) and incorporated into the model as principal ambient controls. While broader meteorological parameters, such as relative humidity, atmospheric pressure, solar radiation, and rainfall, were available, they were not included because the present framework was specifically designed to evaluate direct source-emission relationships rather than atmospheric dispersion processes. Therefore, ambient temperature and wind speed were considered sufficient as the principal meteorological variables influencing combustion conditions and pollutant dispersion.

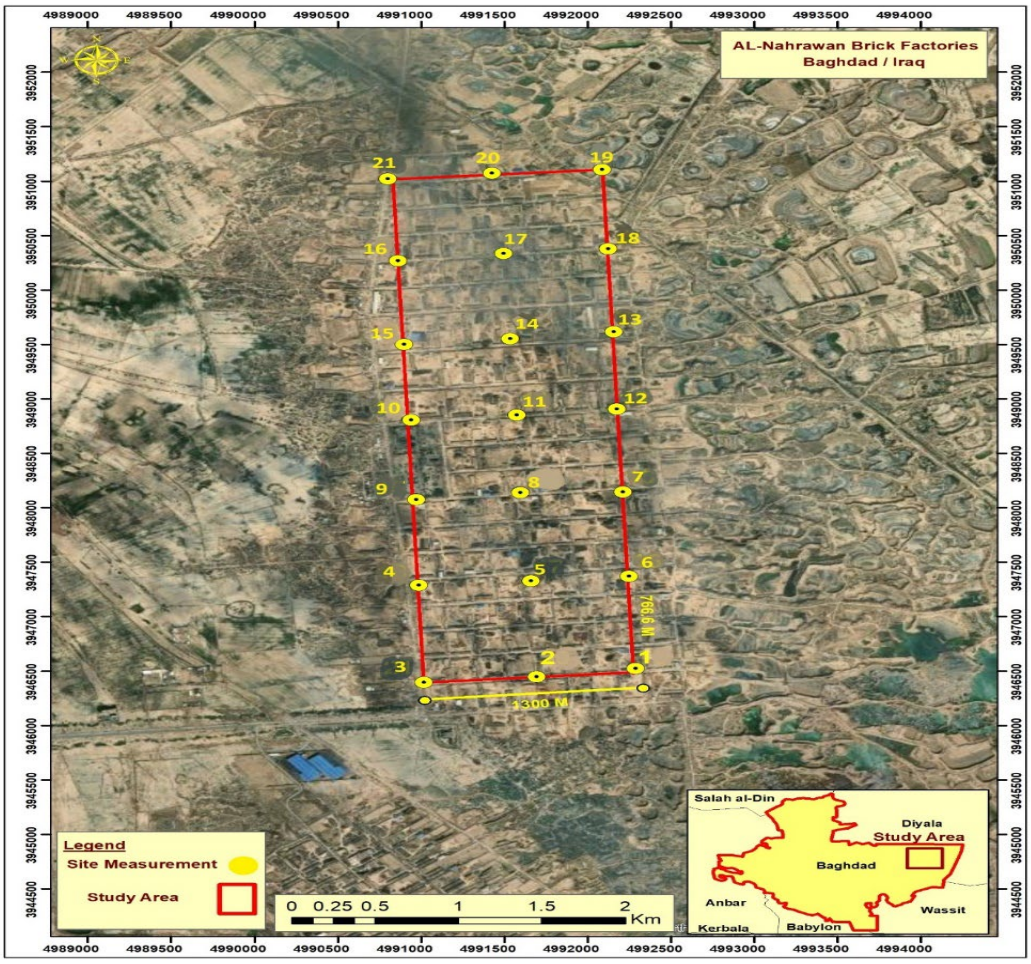


Figure 3: Locations of 21 Measurements Sites Within the Study Area

2.2 Statistical Analysis

The data were entered into IBM SPSS Statistics version 27 for statistical analysis and predictive modelling. The dataset comprised 672 ambient observations collected at 21 monitoring sites across four seasons, with eight observations per site per season. To link the emission inventory with the ambient observations, factories were assigned to predefined areas surrounding the monitoring sites using their geographic coordinates. For each factory, annualised emissions were estimated from the fuel consumption rate corresponding to each season. These estimates represented annual emissions under the operating conditions of the respective season, rather than emissions released during that season alone. For each site and season, the annualised emissions of the associated factories were summed, and the resulting site–season estimate was assigned to the corresponding eight ambient observations. Thus, observations from the same site and season shared the same emission estimate. The CO_2 range of 14.3–665 Gg yr^{-1} reported in Table 1 represents aggregated site-level annualised estimates across sites and seasons, whereas the inventory values of 9.36–14.48 Gg yr^{-1} represent individual-factory annualised estimates. The statistical techniques were selected according to their specific roles within the integrated modelling framework. Spearman rank correlation was initially applied to examine the strength and direction of pairwise associations among ambient air pollutants, estimated greenhouse gas emissions, and meteorological variables without requiring normality. To avoid redundancy arising from the perfect correlations among the estimated CO_2, CH_4, and N_2O emissions, the three gases were combined into carbon dioxide equivalents (CO_2-eq). The 100-year global warming potential (GWP_{100}) values applied were 1 for CO_2, 27.0 for CH_4 from fossil-fuel combustion, and 273 for N_2O, following IPCC AR6 Working Group III, Annex II (IPCC, 2022). CO_2-eq was calculated as $CO_2 + (27.0 \times CH_4) + (273 \times N_2O)$, with all gas emissions expressed in Gg yr^{-1} on the same spatial and temporal basis. The resulting variable was expressed in Gg CO_2-eq yr^{-1}. Because the gas estimates were derived from fuel consumption using fixed emission factors, CO_2-eq was interpreted as a fuel-based emission proxy rather than an independent GHG measurement. Likewise, the perfect correlations among the individual gas estimates reflected their common dependence on fuel consumption. Canonical Correlation Analysis (CCA) was then applied to examine the multivariate relationship between two variable sets. The first set comprised the ambient air pollutants SO_2, NO_2, VOCs, and CO, while the second comprised temperature (T), wind speed (W), and the CO_2-eq fuel-based emission proxy. Principal Component Analysis (PCA) was subsequently applied as a dimensionality-reduction technique before regression modelling. Separate pollutant-specific PCA models were developed for SO_2, NO_2, VOCs, and CO. In each model, the target pollutant was excluded from the PCA predictor set, while the remaining three ambient air pollutants, temperature, wind speed, and the CO_2-eq proxy were included. This prevented the dependent variable from contributing to the principal components subsequently used to predict that same pollutant. The suitability of each predictor dataset for PCA was assessed using the Kaiser–Meyer–Olkin (KMO) measure of sampling adequacy and Bartlett's test of sphericity. The retained principal components were subsequently used as orthogonal predictors in Principal Component Regression (PCR), reducing multicollinearity among the original predictors. Separate PCA-PCR models were fitted to predict the concentrations of SO_2, NO_2, VOCs, and CO. Predictive performance was evaluated using 10-fold cross-validation. Within each fold, PCA was re-estimated using only the training subset, and the retained principal components were used to fit the PCR model. The fitted PCA transformation and regression model were then applied to the corresponding held-out test subset. This procedure was repeated across all ten folds so that each subset served once as the validation set. Predictive performance was assessed using the coefficient of determination (R^2), root mean square error (RMSE), and mean absolute error (MAE), calculated from the held-out predictions.

2.3 Spearman Correlation Coefficient (CC) and Canonical Correlation Coefficient (CCA)

The data collected were analyzed by Spearman CC, the strength and direction of the association between two ranked variables (Shihab, 2022). The canonical correlation determines a linear link between two sets of data with several variables. One set was regarded as a predictor, while the other was considered a response (Figure 4) (Shihab, 2022).

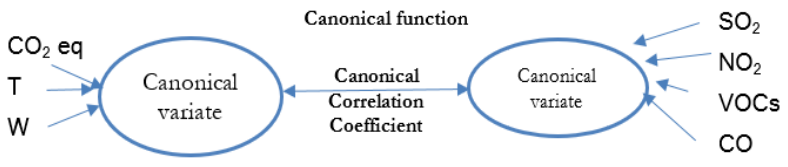


Figure 4: Canonical Function Components

The Spearman correlation analysis provided the preliminary pairwise assessment of relationships among ambient air pollutants, meteorological variables, and CO_2-eq. Because pairwise correlations cannot describe the joint relationship between multidimensional variable groups, CCA was subsequently applied to evaluate the shared multivariate structure between the pollutant set (SO_2, NO_2, VOCs, CO) and the environmental variable set comprising temperature, wind speed, and CO_2-eq.

Principal Component Analysis (PCA) and Principal Component Regression (PCR)

PCA is a data-reduction method that identifies linear combinations of original variables, known as principal components (PCs), which capture the maximum variance in the predictor data while remaining mutually orthogonal (Statheropoulos et al, 1998). In this study, PCA was conducted separately for each pollutant-specific model. The target pollutant was excluded from its corresponding PCA, and the remaining three ambient air pollutants, temperature, wind speed, and CO_2-eq were used as predictors. Two components with eigenvalues greater than 1 were retained in each model and subsequently entered into PCR (Pasic et al, 2023; Song et al, 2020)

$$C_p = \beta_0 + \sum_{i=1}^{k} \beta_i PC_i \quad (1)$$

Where:

C_p = Pollutants concentration,

β_0 = Constant , i = 1, 2, … n,

k = Count of principal components,

β_i = PCA regression coefficient ,

PC_i = Principal components from PCA

3. RESULTS AND DISCUSSION

3.1 Greenhouse Gases Emissions (Inventory) Levels

The analysis of oil consumption in the brick industry focused on fuel usage and GHGs emissions, utilizing IPCC inventory software to quantify emissions of CO_2, CH_4, and N_2O from production processes. The study found that 75% of brick factories consume an average of 247 cubic metres per month (m^3/month) of fuel, while 5% of that factories use 382 m^3/month of fuel, as shown in Figure 5a, with CO_2 emissions directly correlated to fuel consumption; factories using 382 m^3/month emit approximately 14.48 gigagrams (Gg) of CO_2, compared to 9.36 Gg from those using 247 m^3/month, with the emission factor for carbon dioxide is 77400 Kilograms of carbon dioxide emitted per terajoule of fuel energy consumed (kg CO_2/TJ) (IPCC, 2006), as shown in Figure 5b. CH_4 peaked at 0.00056 Gg for the higher fuel consumption and dropped to 0.00036 Gg for the lower, and the emission factor of CH_4 is 3 Kg CH_4/TJ (IPCC, 2006), as shown in Figure 5c. While N_2O also showed a similar trend 0.00011 Gg and 0.00007 Gg for the maximum and minimum respectively, as shown in Figure 5c when the value of the emission factor is 0.3 Kg N_2O /TJ(IPCC, 2006), indicating a clear relationship between fuel usage and emissions in the Al-Nahrawan industrial area's brick industry (Levermore, 2008). Fossil fuel combustion and alternative energy use emit GHGs that add to the global warming effect, and other pollutants, into the atmosphere. Heavy fuel oil combustion during the brick firing stage was determined as the main source for the combustion air pollutant and GHG emissions. Emissions of CO and VOCs were largely due to incomplete combustion while the amount of sulphur in the fuel was the main source of SO_2 emissions. Thus, there is potential to significantly reduce pollutant emissions and improve the air quality in the local area by improving combustion efficiency, using lower sulphur or cleaner fuels, optimising the operation and maintenance of the kilns and the deployment of appropriate emission control technologies (Yousefi et al, 2016).

Natural Resources for Human Health
eISSN: 2583-1194

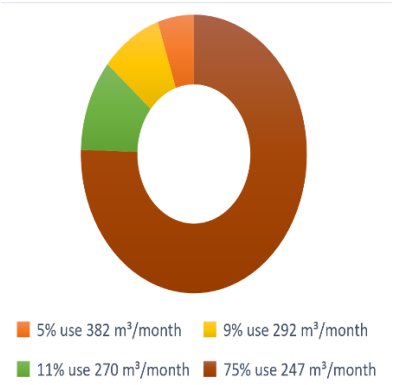


Figure 5a: Percentage of Factories that Share Fuel per Month in m³/month

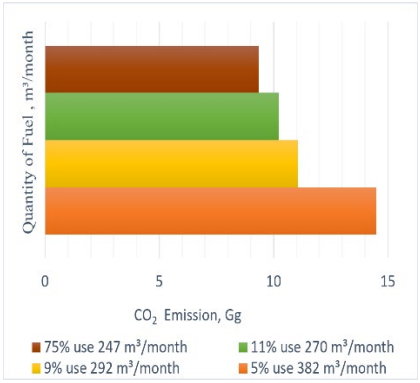


Figure 5b: CO_2 Emissions Amount in Gg Estimation Using IPCC Inventory Software 2006

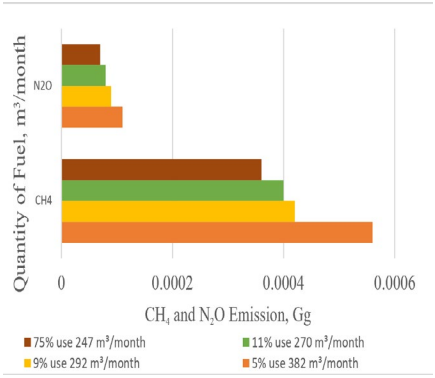


Figure 5c: CH_4 and N_2O Emissions Amount in Gg Estimation Using IPCC Inventory Software 2006

This study demonstrates that brick production in the Al-Nahrawan industrial zone significantly contributes to GHGs emissions and air pollution, aligning with global evidence on the environmental impact of traditional brick-making processes (Valdes et al ,2020; Seay et al, 2021). The estimated CO_2 emissions ranging from 9.36 Gg to 14.48 Gg confirm that heavy fuel oil combustion is a major source of GHGs, consistent with IPCC reports on fossil fuel-driven emissions (IPCC, 2013). Methane and nitrous oxide emissions, though smaller in magnitude, are critical due to their high global warming potential, reinforcing the need for comprehensive mitigation strategies.

3.2 Air Pollutants Concentrations Level

As shown in Table 1, the ambient air-pollutant measurements showed substantial variability among the monitored gases. Mean concentrations of SO_2, NO_2, and CO were 0.216 ppm, 0.190 ppm, and 40.59 ppm, respectively, while VOC concentrations were comparatively lower. In contrast, CO_2, CH_4, and N_2O were not measured as ambient concentrations but were estimated as greenhouse gas emissions using the IPCC inventory approach and are therefore reported separately in Gg. Consequently, direct numerical comparison between the measured pollutant concentrations (ppm) and the estimated GHG emissions (Gg) is not appropriate.

Table 1: The Statistical Description of Air Pollutants and GHG Emissions

Pollutants		Mean	Standard deviation (SD)	Minimum	Maximum
Air pollutants	SO_2 (ppm)	0.216	0.149	0.002	0.743
	NO_2 (ppm)	0.190	0.150	0.041	0.970
	VOCs (ppm)	0.105	0.066	0.003	0.329
	CO (ppm)	40.586	12.183	18.00	77.00
GHG	CO_2 (Gg)	209.475	158.703	14.330	665.076
	CH_4 (Gg)	0.008	0.006	0.0006	0.026
	N_2O (Gg)	0.001	0.001	0.0001	0.0052

SO_2 concentrations exhibited clear seasonal variation, with an annual average of 0.216 ppm across all sites. The highest site-level seasonal mean concentration (0.48 ppm) occurred during summer at Site 11, exceeding both the Iraqi standard (0.15 ppm) and the WHO guideline value (0.015 ppm). Figure 6 shows that SO_2 levels were lowest in the winter (0.097 ppm at Site 1), rose slowly in the spring, and then rose quickly in the summer, when almost all sites went over the limits. Although concentrations declined in autumn, several locations remained above the standards. The pronounced summer peak was attributed to high

temperatures, low wind speeds, and full-capacity kiln operations, which together reduce atmospheric dispersion and intensify emissions from heavy fuel oil combustion. Heavy fuel oil contains a high concentration of sulphur (Ministry of oil, 2024). So, when it is burned in traditional brick kilns to produce energy, the sulphur is oxidized and emitted to the atmosphere. Exceedance of both Iraqi and WHO guideline levels indicates a potential risk to neighboring populations and workers exposed to pollutants from brick kiln activities. Prolonged exposure to elevated SO_2 levels can result in respiratory system irritation, decreased lung function, and exacerbation of asthma and other chronic respiratory illnesses. Environmentally SO_2 emissions are also responsible for acid deposition that can damage soil quality, plants and nearby ecosystems (WHO, 2021).

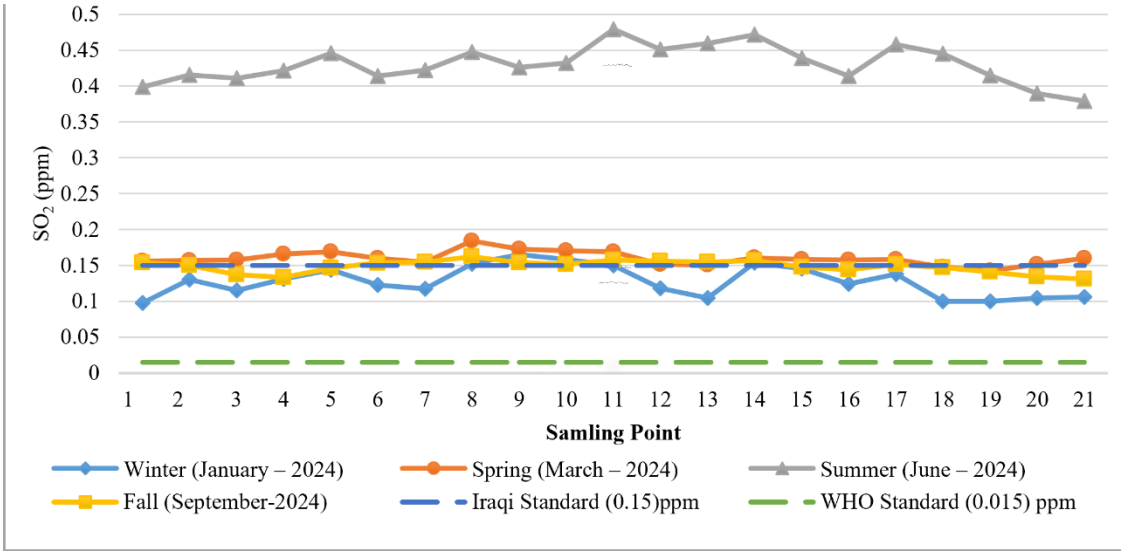


Figure 6: Average Concentrations of SO_2 in Al- Nahrawan Industrial Area During Four Seasons for 21 Sites

NO_2 concentrations exceeded the WHO guideline value (0.013 ppm) at all sites and the Iraqi standard (0.1 ppm) at all sites during summer, with a peak site-level seasonal mean of 0.48 ppm (Figure 7). In combustion sources, NO_x is formed mainly through the thermal mechanism, which is favoured by high flame temperatures, and through oxidation of fuel-bound nitrogen, which is relatively abundant in residual heavy fuel oil. Nitric oxide emitted from the kilns is rapidly oxidized to NO_2 in the atmosphere, so the high summer NO_2 levels are consistent with intensive kiln firing combined with strong photochemical activity. Elevated NO_2 exposure can aggravate respiratory disease, particularly in children, the elderly and people with pre-existing respiratory conditions, and NO_2 also contributes to the formation of ground-level ozone and secondary fine particulate matter (WHO, 2021; EPA, 2024).

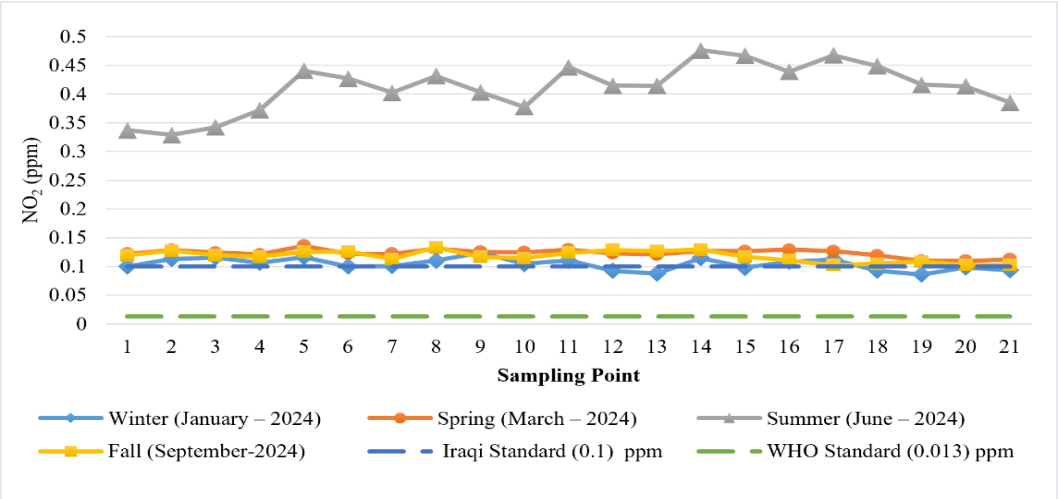


Figure 7: Average Concentrations of NO_2 in Al- Nahrawan Industrial Area During Four Seasons for 21 Sites

VOCs and hydrocarbon pollutants, primarily invisible, were measured at various sites, with the highest concentration recorded at 0.23 ppm during summer at site 8 and the lowest at 0.0195 ppm in winter at site 7, as shown in Figure 8. Although WHO and Iraqi standards do not specify VOC limits, the emphasis is on minimizing these substances, which often emit strong odors due to their prevalence in industrial areas and the use of heavy fuels oil. Insufficient oxygen during the combustion of heavy fuel oil in brick kilns leads to the emission of large quantities of VOCs into the atmosphere. Traditional kilns used in brick manufacturing are the primary cause of high VOCs concentrations in the atmosphere during fuel combustion, primarily because they lack sufficient oxygen to complete the process. Exposure to VOCs can lead to serious health issues, including liver and kidney damage, respiratory irritation, headaches, and central nervous system effects (Xin et al, 2022). High concentrations of VOC are environmentally relevant since many VOC species are involved in photochemical processes which lead to the generation of ground level ozone. Some VOCs have also been linked to detrimental health consequences with long-term exposure, including neurological damage and an increased risk of certain malignancies, depending on the chemical makeup of the released molecules (EPA, 2024).

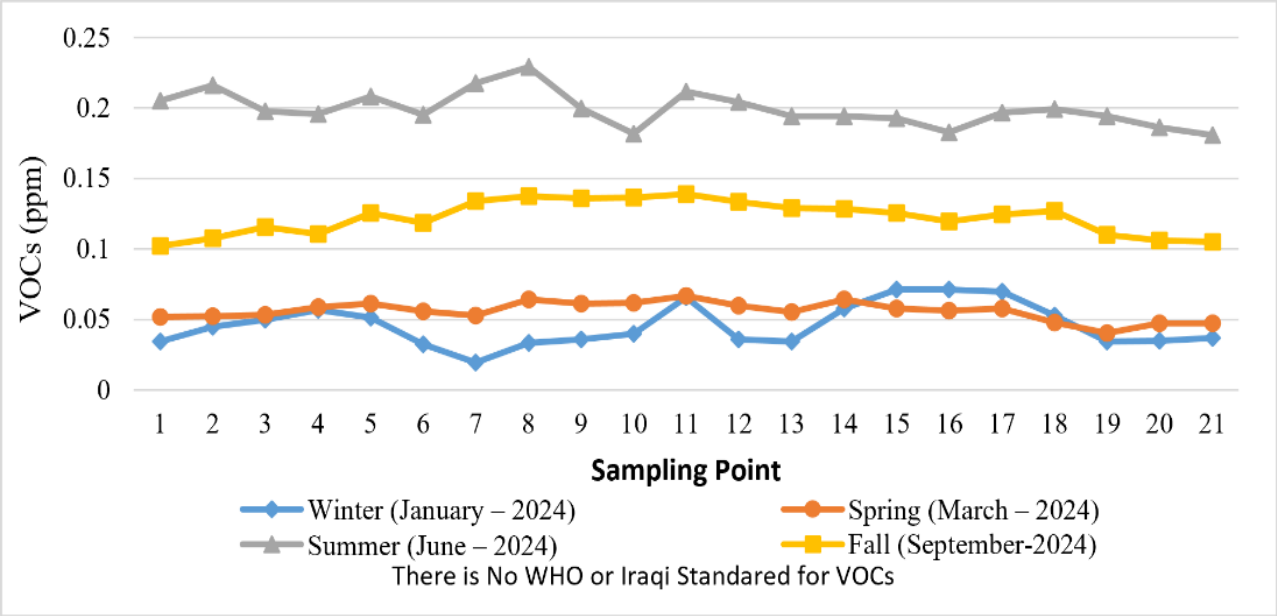


Figure 8: Average Concentrations of VOCs in Al- Nahrawan Industrial Area During Four Seasons for 21 Sites.

In 2024, CO levels were monitored at 21 sites throughout the year. In 2024, outdoor CO concentrations were monitored at 21 sites within the Al-Nahrawan brick manufacturing area. The monitoring locations were situated along kiln smoke-plume pathways; therefore, the measurements represented local air affected by industrial emissions rather than regional background air quality. Revealing that most locations exceeded the World Health Organization (WHO) and Iraqi standard limits of 3.5 ppm and 35 ppm, respectively, with a peak concentration of 61.25 ppm recorded in summer at site No. 14. The lowest level, 24.25 ppm, was observed in winter at site No. 20, which is within acceptable Iraqi limits but out of WHO limits, as shown in Figure 9. The primary cause of elevated CO concentrations is attributed to the incomplete combustion of high-density heavy fuel oil in brick factory kilns, where inadequate temperature control and oxygen supply lead to significant CO emissions. Elevated amounts of CO can decrease the blood's capacity to carry oxygen by forming carboxyhemoglobin and may cause headaches, dizziness, exhaustion, and cardiovascular stress from prolonged exposure. These results imply a possibility of increasing health risks for workers and communities in the vicinity during periods of high brick production (WHO,2021).

Natural Resources for Human Health
eISSN: 2583-1194

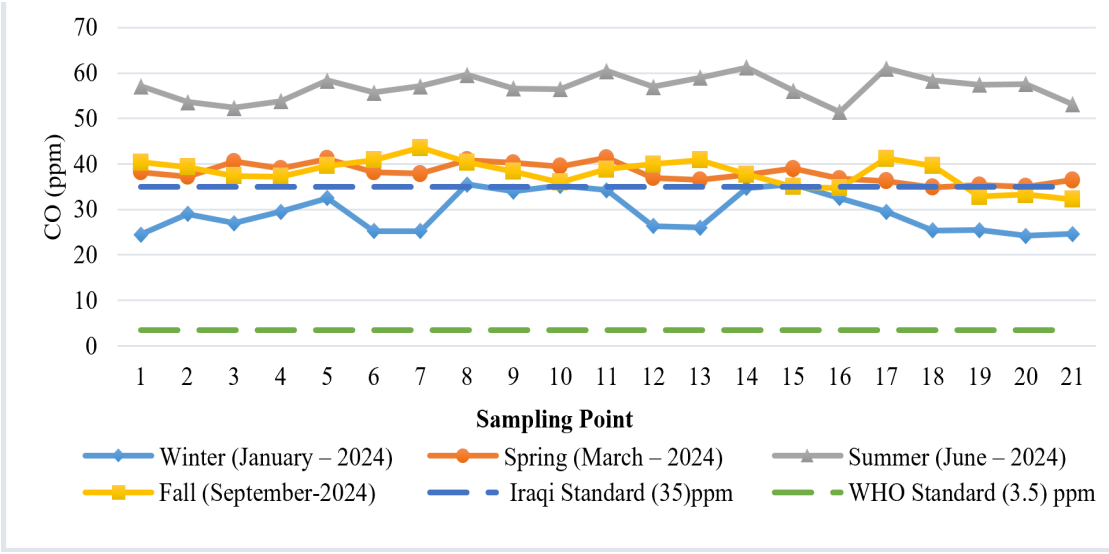


Figure 9: Average Concentrations of CO in Al- Nahrawan Industrial Area During Four Seasons for 21 Sites

These ambient air quality measurements revealed that SO_2 and NO_2 concentrations frequently exceeded Iraqi standards, particularly during summer when temperatures exceeded 40 degrees Celsius (°C) and wind speeds were low. These findings corroborate previous studies indicating that high temperatures and stagnant air conditions exacerbate pollutant accumulation (Song et al, 2020). The strong seasonal variation observed for VOCs and CO further highlights the influence of combustion efficiency and meteorological factors. High levels of CO, which reach 61.25 ppm, show that heavy fuel oil is not burning completely. This is a common problem in brick kiln operations in South Asia and the Middle East (Haque et al, 2022; Weyant et al, 2016).

3.3 Statistical modelling

3.3.1 Spearman CC and CCA between air pollutants and GHGs

The initial Spearman correlation analysis indicated clear and statistically significant positive relationships among the main ambient air pollutants. The strongest correlation was observed between SO_2 and NO_2 ($r = 0.837$, $p < 0.01$), followed by VOCs and CO, suggesting common emission sources and similar atmospheric behaviour. Temperature (T) was moderately to strongly correlated with most pollutants, particularly VOCs ($r = 0.857$), reflecting the influence of thermal conditions on pollutant variability. In contrast, wind speed (W) showed generally weak correlations with the studied variables, indicating a limited monotonic association within the observed dataset. Moderate positive correlations were also observed between the ambient air pollutants and the individually estimated GHGs ($r = 0.328$–0.409). Notably, CO_2, CH_4, and N_2O exhibited perfect positive correlations with one another ($r = 1.000$). These perfect correlations are mathematical consequences of estimating the three GHGs from the same fuel-consumption activity data using fixed Tier 1 emission factors and therefore should not be interpreted as evidence that independently measured GHGs exhibited identical environmental behaviour. Accordingly, CO_2, CH_4, and N_2O were retained as separate variables in this initial Spearman correlation analysis to examine their individual pairwise relationships with the ambient air pollutants and meteorological variables. To avoid redundant GHG information in the subsequent multivariate analyses, the three estimated GHGs were subsequently converted into a single carbon dioxide-equivalent (CO_2-eq) indicator. Figure 10 illustrates the Spearman correlation heat map of the ambient air pollutants, individually estimated GHGs, and meteorological variables.

Natural Resources for Human Health
eISSN: 2583-1194



Figure 10: The Heatmap of Spearman's rank CC Among the Air Pollution Parameters and GHG

The Spearman correlation analysis revealed statistically significant relationships among ambient air pollutants, meteorological variables, and the integrated greenhouse gas indicator (CO_2-eq). Among the measured environmental variables, the strongest positive correlation was observed between temperature and VOCs (r = 0.857), followed by SO_2 and NO_2 (r = 0.837) and NO_2 and CO (r = 0.827). These strong associations indicate substantial covariation among several ambient air pollutants and between pollutant concentrations and thermal conditions. Wind speed showed comparatively weak correlations with the measured ambient air pollutants, with correlation coefficients ranging from r = 0.048 to 0.153, suggesting a limited monotonic association within the observed dataset. In contrast, CO_2-eq showed positive correlations with SO_2 (r = 0.365), NO_2 (r = 0.328), VOCs (r = 0.408), and CO (r = 0.387) as shown in Figure 11. The strongest association with CO_2-eq was therefore observed for VOCs, although the pollutant–CO_2-eq correlations were generally moderate in magnitude. Overall, the Spearman results demonstrate that ambient air pollutant concentrations were significantly associated with both meteorological conditions and the integrated GHG indicator. The particularly strong relationship between temperature and VOCs highlights the importance of seasonal and thermal conditions, whereas the positive associations between CO_2-eq and the measured pollutants indicate that higher estimated climate-related emissions generally coincided with higher ambient pollutant concentrations.

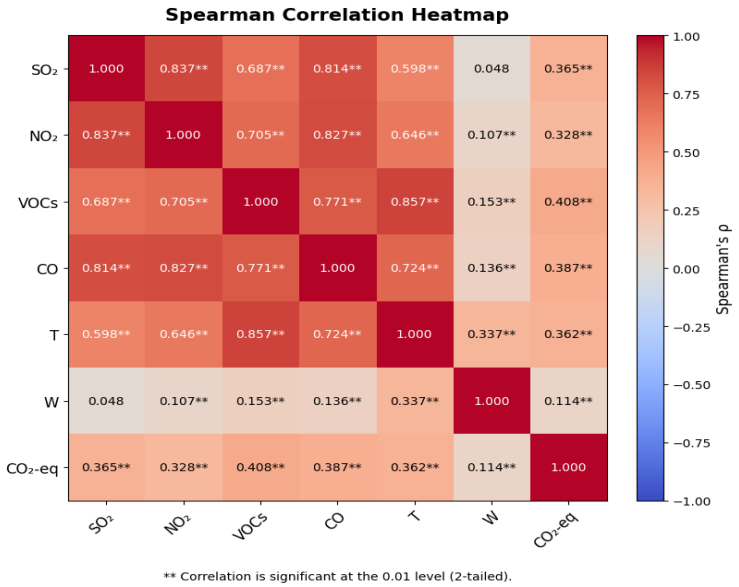


Figure 11: Correlation Heat Map with all Obtained Air Pollution Parameters and CO_2-eq From the Sample.

Canonical correlation analysis identified a strong and statistically significant multivariate association between the ambient air pollutants (SO_2, NO_2, VOCs, and CO) and the environmental variables represented by temperature, wind speed, and CO_2-eq. Interpretation focused on the first canonical function because it represented the dominant relationship between the two variable sets. The first canonical correlation was 0.878, while Wilks' Lambda ($\Lambda = 0.220$, $F = 113.085$, $p < 0.001$) confirmed the statistical significance of the multivariate association. Within the pollutant set, VOCs showed the strongest canonical loading (−0.996), followed by CO (−0.776), NO_2 (−0.680), and SO_2 (−0.678). Within the environmental variable set, temperature exhibited the strongest loading (−0.989), followed by CO_2-eq (−0.468), whereas wind speed showed a comparatively weak loading (−0.142). These findings indicate that the dominant canonical relationship was primarily characterized by the association between the overall ambient air pollution pattern and environmental conditions dominated by temperature, with an additional contribution from CO_2-eq. The first environmental canonical variate explained approximately 48.5% of the variance in the ambient air pollutant set, while the first pollutant canonical variate explained approximately 31.3% of the variance in the environmental variable set. Table 2 presents the canonical correlation results.

Table 2: Results of the First Canonical Function Between Ambient Air Pollutants and Environmental Variables.

Canonical correlations						
Correlation	**Eigen value**	**Wilks Statistic**	**F**	**Num D.F.**	**Denom D.F.**	**Sig.**
0.878	3.354	0.220	113.085	12.000	1759.716	0.000

Correlation coefficients		**Set 1 Canonical loadings**		**Set 2 Canonical loadings**	
Variable	**1**	**Variable**	**1**	**Variable**	**1**
SO_2	-0.039	SO_2	-0.678	T	-0.989
NO_2	0.158	NO_2	-0.680	W	-0.142
VOCs	-1.078	VOCs	-0.996	CO_2 eq	-0.468
CO	-0.009	CO	-0.776		

proportion of variance explained		
Canonical variable	**Set 1 by Set 2**	**Set 2 by Set 1**
1	0.485	0.313

Overall, the CCA demonstrated a strong and statistically significant multivariate association between ambient air pollutants and the combined environmental conditions represented by temperature, wind speed, and CO_2-eq. The loading structure indicates that the first canonical relationship was characterized principally by VOCs within the pollutant set and temperature within the environmental set, with CO_2-eq providing an additional moderate contribution. These results complement the Spearman analysis by showing that pollutant variability is associated not only with individual pairwise relationships but also with the combined multivariate environmental structure.

3.3.2 Principal Component Regression (PCR) for Air Pollutant and GHGs

Principal Component Analysis (PCA) was conducted separately for each pollutant-specific model, with the target pollutant excluded from its corresponding predictor set. The suitability of the predictor datasets for PCA was confirmed by Kaiser–Meyer–Olkin (KMO) values of 0.783, 0.783, 0.786, and 0.726 for the SO_2, NO_2, VOCs, and CO models, respectively. Bartlett's test of sphericity was statistically significant for all four models ($p < 0.001$), confirming sufficient intercorrelations among the predictor variables for PCA (Table 3). Two principal components with eigenvalues greater than 1 were retained for each pollutant-specific model. Together, PC1 and PC2 explained 75.172% of the total predictor variance for SO_2, 75.155% for NO_2, 74.475% for VOCs, and 75.661% for CO. Across the four models, PC1 accounted for 55.914–57.741% of the total variance and was characterized by high positive loadings of the remaining ambient air pollutants and temperature, together with a

moderate positive contribution from CO_2-eq. For example, in the SO_2 model, PC1 showed high loadings for VOCs (0.942), CO (0.885), temperature (0.872), and NO_2 (0.831), while CO_2-eq showed a moderate loading of 0.556. Similar loading patterns were observed across the other pollutant-specific models. Accordingly, PC1 was interpreted as a Pollution–Combustion Intensity Component, representing the common variability associated with combustion-related pollutant levels and thermal conditions, with an additional contribution from the integrated GHG indicator. In contrast, PC2 accounted for approximately 17.430–18.561% of the total variance and was consistently dominated by wind speed, with loadings of 0.956, 0.967, 0.922, and 0.916 in the SO_2, NO_2, VOCs, and CO models, respectively. PC2 was therefore interpreted as a Meteorological Dispersion Component, primarily representing atmospheric transport and dispersion conditions. The summarized PCA structure is presented in Table 5.

The retained principal components were subsequently used as orthogonal predictors in the pollutant-specific Principal Component Regression (PCR) models. As presented in Table 4, the developed models demonstrated satisfactory explanatory performance, with R^2 values of 0.707, 0.713, 0.776, and 0.695 and adjusted R^2 values of 0.706, 0.712, 0.775, and 0.694 for SO_2, NO_2, VOCs, and CO, respectively. All four regression models were statistically significant ($p < 0.001$). The VOCs model showed the highest explanatory performance, accounting for 77.6% of the observed variability, whereas the CO model showed the lowest but still satisfactory explanatory performance ($R^2 = 0.695$). The predictive reliability of the developed models was further evaluated using 10-fold cross-validation. As presented in Table 6, the mean cross-validated R^2 values were 0.828, 0.859, 0.850, and 0.680 for SO_2, NO_2, VOCs, and CO, respectively. The corresponding mean RMSE values were 0.058, 0.054, 0.025, and 6.741, while the mean MAE values were 0.035, 0.034, 0.018, and 5.410, respectively. The NO_2 model achieved the highest mean cross-validated R^2, followed by VOCs, SO_2, and CO. Overall, the cross-validation results support the predictive stability of the developed models within the available dataset. PCR was particularly appropriate for the present dataset because it reduced multicollinearity by transforming correlated environmental predictors into orthogonal principal components before regression modelling. This improved coefficient stability and enabled the common variability among ambient pollutants, meteorological conditions, and CO_2-eq to be incorporated without directly regressing on highly correlated original predictors. The findings are consistent with previous applications of multivariate statistical techniques in air-quality modelling (Song et al, 2020; Pasic et al, 2023; Moradi et al, 2024). Overall, the developed PCA-PCR framework demonstrated satisfactory explanatory and predictive performance for ambient pollutant concentrations within the Al-Nahrawan Industrial Area.

Table 3: KMO and Bartlett's Test for the Suitability of Data for Principal Component Analysis (PCA)

Variable		**SO_2**	**NO_2**	**VOCs**	**CO**
Kaiser-Meyer-Olkin Measure of Sampling Adequacy (KMO)		0.783	0.783	0.786	0.726
Bartlett's Test of Sphericity	**Approx. Chi-Square**	2487.384	2464.264	2424.730	2903.380
	df	15	15	15	15
	P	<0.001	<0.001	<0.001	<0.001

Table 4: Validation Results of PCR for Air Pollutants

Contaminant	**Number of samples**	**R^2**	**Adjusted R^2**	**Standard error (SE) of estimate**	**F value**	**P- value**
SO_2	672	0.707	0.706	0.0808	808.243	<0.001
NO_2	672	0.713	0.712	0.0807	829.347	<0.001
VOCs	672	0.776	0.775	0.0314	1156.2	<0.001
CO	672	0.695	0.694	6.742	761.324	<0.001

Table 5: Summary of Principal Component Analysis of Air Pollutants

Component	Initial Eigen values			Component matrix		
	Total	% of variance	Cumulative%	variable	PC1 loading	PC2 loading
PC1	3.355–3.464	55.914–57.741	55.914–57.741	SO_2	0.873–0.900	−0.052–0.152
PC2	1.046–1.114	17.430–18.561	74.475–75.661	NO_2	0.831–0.882	−0.049–0.195
				VOCs	0.927–0.942	0.041–0.221
				CO	0.858–0.885	0.148–0.233
				T	0.848–0.872	−0.246–−0.210
				W	−0.165–−0.104	0.916–0.967
				CO_2 eq	0.537–0.568	−0.545– - 0.476

Table 6: Performance Evaluation of the Developed Predictive Models Using 10-Fold Cross Validation

Pollutant	Mean Cross-Validated R^2	Mean RMSE	Mean MAE
SO_2	0.828	0.058	0.035
NO_2	0.859	0.054	0.034
VOCs	0.850	0.025	0.018
CO	0.680	6.741	5.410

For gaseous pollutants (SO_2, NO_2, VOCs, and CO), the developed PCA-PCR models demonstrated satisfactory predictive performance, with close agreement between predicted and observed pollutant concentrations. The scatterplots in Figure 12 showed clear linear agreement between predicted and observed values. The coefficients of determination (R^2 = 0.695–0.776) indicated that the models explained a substantial proportion of the variability in pollutant concentrations. In addition, 10-fold cross-validation supported the predictive stability of the models, with mean cross-validated R^2 values ranging from 0.680 to 0.859. Some dispersion at higher concentrations may reflect variations in meteorological conditions and emission intensity. Similar behaviour has been reported in air-quality forecasting studies, where temperature, wind speed, and emission variability can influence predictive performance (Lee & Chen, 2026). Overall, the PCA-PCR approach provides a useful framework for pollutant prediction and air-quality assessment while minimizing multicollinearity among environmental predictors.

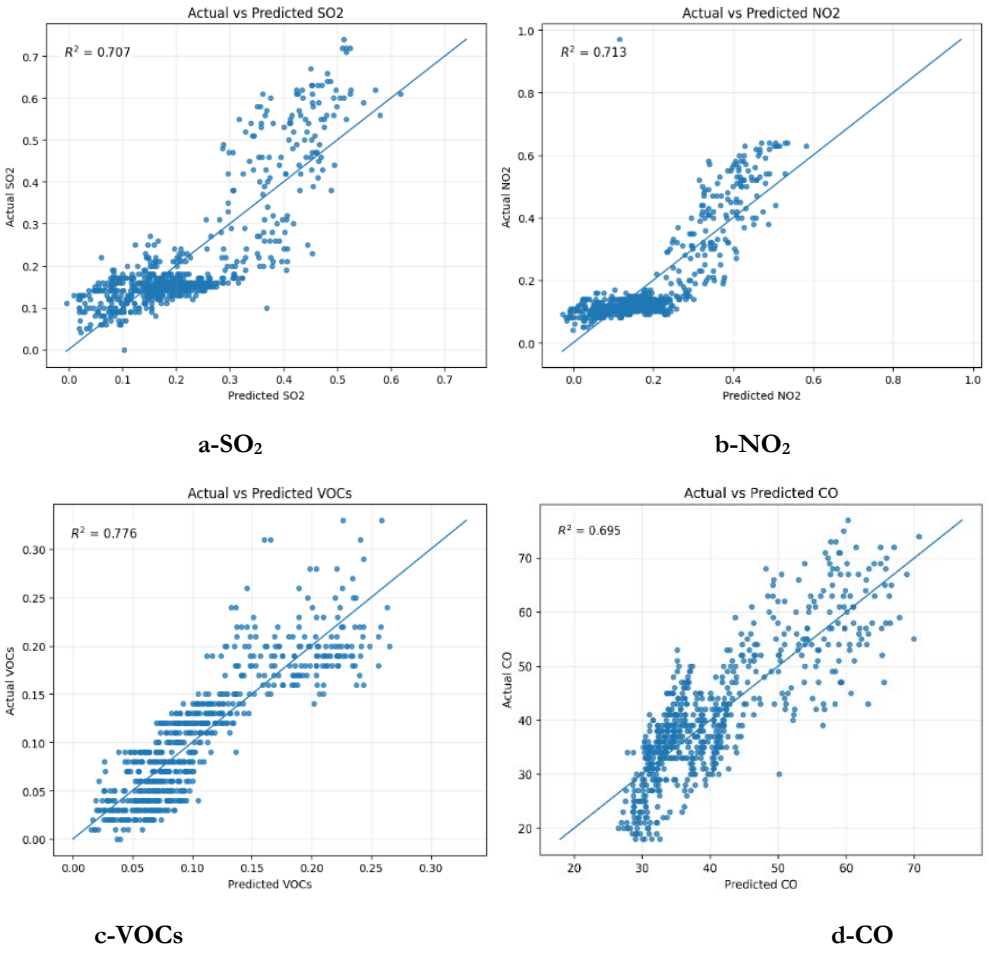


Figure 12: PCR Model Validation: Actual vs. Predicted

The pollutant-specific PCA-PCR regression models are summarized comparatively in Table 7. The table presents the regression equations together with the unstandardized coefficients (B), standardized coefficients (β), statistical significance, and 95% confidence intervals for the retained principal components. Presenting the four models within a single table facilitates direct comparison of the magnitude and direction of the effects of PC1 and PC2 across the target pollutants.

As shown in Table 7, PC1 was consistently the dominant predictor across all four pollutant models, with standardized regression coefficients (β) ranging from 0.828 to 0.852. The highest PC1 coefficient was observed for VOCs (β = 0.852), followed by NO_2 (β = 0.834), CO (β = 0.832), and SO_2 (β = 0.828), with all PC1 coefficients being statistically significant ($p < 0.001$). This consistent pattern indicates that the common pollution– Combustion Intensity Component represented by PC1 were strongly associated with variability across all four target pollutants.

In contrast, PC2 showed pollutant-specific differences in both magnitude and direction. Significant negative coefficients were observed for SO_2 (β = −0.149, $p < 0.001$) and NO_2 (β = −0.128, $p < 0.001$), whereas positive coefficients were observed for VOCs (β = 0.224, $p < 0.001$) and CO (β = 0.049, $p = 0.022$). The largest absolute PC2 coefficient was observed for VOCs, whereas CO exhibited the smallest. Given that PC2 was predominantly characterized by wind speed, these differences suggest pollutant-specific associations with meteorological dispersion and transport conditions. The positive coefficients observed for VOCs and CO should not be interpreted as evidence that increasing wind speed directly increases their emissions; rather, they indicate statistical associations with the wind-dominated component that may reflect atmospheric transport and spatial redistribution within the study area. Overall, PC1 showed a consistently strong association across all four pollutant models, whereas PC2 exhibited weaker and pollutant-specific associations.

The contrasting PC2 coefficients likely reflect pollutant-specific atmospheric transport behavior. The negative coefficients for

SO_2 and NO_2 are consistent with enhanced atmospheric dilution and dispersion under stronger wind conditions. The importance of wind speed, wind direction, and atmospheric conditions in controlling the dispersion and spatial distribution of combustion-related pollutants has also been demonstrated under Iraqi industrial conditions (Nasser et al, 2024). In contrast, the positive PC2 coefficient for VOCs may reflect wind-associated transport and spatial redistribution within the industrial area rather than increased VOC generation. Mai et al. (2024) reported substantial spatial variability in VOC concentrations within an industrial zone and demonstrated that their spatiotemporal variations were influenced by both industrial emissions and meteorological conditions. Although volatilization and the spatial arrangement of emission sources may also contribute to VOC variability, the present dataset cannot distinguish their individual contributions. Therefore, the positive VOC–PC2 association should be interpreted cautiously as a meteorologically influenced transport relationship rather than a direct causal effect of wind speed on VOC emissions.

Table 7: Comparative Summary of PCA-PCR Regression Models for Ambient Air Pollutants

Pollutant	Regression equation	Predictor	B	SE	β	t	p-value	95% CI for B
SO_2	$SO_2 = 0.216 + 0.123(PC1) - 0.022(PC2)$	Constant	0.216	0.003	—	69.418	<0.001	0.210–0.223
		PC1	0.123	0.003	0.828	39.567	<0.001	0.117–0.130
		PC2	−0.022	0.003	−0.149	−7.139	<0.001	−0.028 to −0.016
NO_2	$NO_2 = 0.191 + 0.125(PC1) - 0.019(PC2)$	Constant	0.191	0.003	—	61.198	<0.001	0.184–0.197
		PC1	0.125	0.003	0.834	40.254	<0.001	0.119–0.132
		PC2	−0.019	0.003	−0.128	−6.192	<0.001	−0.025 to −0.013
VOCs	VOCs = 0.106 +0.056(PC1) +0.015(PC2)	Constant	0.106	0.001	—	87.403	<0.001	0.103–0.108
		PC1	0.056	0.001	0.852	46.506	<0.001	0.054–0.059
		PC2	0.015	0.001	0.224	12.230	<0.001	0.012–0.017
CO	CO=40.586 +10.138(PC1) + 0.598(PC2)	Constant	40.586	0.260	—	156.065	<0.001	40.076–41.097
		PC1	10.138	0.260	0.832	38.953	<0.001	9.627–10.649
		PC2	0.598	0.260	0.049	2.299	0.022	0.087–1.109

3.4 Uncertainty Analysis

It is recognized that the predictive performance of environmental forecasting models may be influenced by both model uncertainty and measurement uncertainty. The uncertainty in the measurement could be due to the precision of the instrument, the calibration methods, the seasonal variability of the meteorology and the spatial heterogeneity of the monitoring locations.

To reduce these uncertainties, all instruments were calibrated before the field measurements, standard sample protocols were followed, and repeated measurements were made at 21 monitoring sites in four seasons.

Model uncertainty was evaluated using multiple statistical performance indicators, including R^2, adjusted R^2, RMSE, ANOVA, residual diagnostic analysis, observed-versus-predicted comparisons, 95% confidence intervals for the regression coefficients, and 10-fold cross-validation. The validation results demonstrated satisfactory predictive performance and statistical robustness of the developed PCA-PCR models for the analysed dataset. The 10-fold cross-validation provided an internal assessment of model stability and generalizability across different subsets of the available data. However, external validation using independent datasets was beyond the scope of the present study because the proposed modelling framework was developed using field data collected from the Al-Nahrawan brick manufacturing area. Therefore, future studies are recommended to evaluate the transferability and generalizability of the proposed models using independent datasets from other brick manufacturing areas. Recent studies have also highlighted the significance of quantifying uncertainty, clear validation procedures, and independent model evaluation to improve the scientific credibility and practical use of environmental forecasting models (Shao et al, 2026).

4. CONCLUSION

The principal contribution of this study is the integration of GHG emission estimation, ambient air-quality assessment, and multivariate statistical modelling into a unified framework for evaluating the environmental impacts of brick manufacturing. The combined use of correlation analysis, CCA, PCA, and PCR provided an integrated assessment of the relationships among ambient air pollutants, CO_2-eq, and meteorological variables while reducing multicollinearity and supporting pollutant prediction. The findings demonstrated substantial GHG emissions associated with heavy fuel-oil consumption and elevated concentrations of SO_2, NO_2, VOCs, and CO, particularly during summer. The statistical analyses further demonstrated significant relationships among ambient pollutants, CO_2-eq, and meteorological conditions. PCA effectively reduced the correlated predictor structure into orthogonal components, while the developed PCA-PCR models showed satisfactory explanatory and predictive performance for the four ambient pollutants. The models were internally validated using 10-fold cross-validation, supporting their predictive stability within the analysed dataset. Overall, the proposed framework provides a practical approach for supporting air-quality assessment, pollutant prediction, environmental monitoring, and evidence-based decision-making in brick manufacturing areas. The findings emphasize the importance of cleaner fuels, improved combustion efficiency, technological modernization, and strengthened environmental monitoring and regulation. Future studies should incorporate additional operational and meteorological variables, continuous monitoring data, and external validation using independent datasets from other brick manufacturing areas. More advanced machine-learning approaches may also be investigated to capture nonlinear relationships and further improve predictive performance.

ACKNOWLEDGMENT

This study did not obtain any specific financing from public, commercial, or non-profit entities.

AUTHOR CONTRIBUTIONS

Sarah Duraid: Methodology, Investigation, Data curation, Formal analysis, Validation, Writing -original draft conducted the experimental work and wrote the manuscript; Noor Faizah Fitri: Supervision, conceptualization, contributed to the research idea, and reviewed the manuscript

CONFLICT OF INTEREST

The authors declare that there is no conflict of interest regarding the publication of this manuscript. In addition, ethical issues, including plagiarism, informed consent, misconduct, data fabrication and/or falsification, double publication and/or submission, and redundancy, were observed by the authors.

ETHICS STATEMENT

Not applicable. This study did not involve human participants or animals.

DATA AVAILABILITY STATEMENT

The datasets generated and/or analyzed during the current study are available from the corresponding author upon reasonable request.

REFERENCES

[1] Al-Nuzal, S.M.D.; Al-Bakri, S.A.; Zankana, S.D.A., (2018). Environmental impact assessment for brick factory in Baghdad, Iraq. Eng. Technol. J., 36(1C): 38–48 (11 pages).

[2] Afifa ,Arshad, K.; Hussain, N.; Ashraf, M.H.; Saleem, M.Z., (2024). Air pollution and climate change as grand challenges to sustainability. Sci. Total Environ., 928: 172370. https://pubmed.ncbi.nlm.nih.gov/38604367/

[3] Castelli, M.; Clemente, F.M.; Popovič, A.; Silva, S.; Vanneschi, L., (2020). A machine learning approach to predict air quality in California. Complex., 2020: 8049504. https://onlinelibrary.wiley.com/doi/full/10.1155/2020/8049504

[4] Chien, F. S., Chau, K. Y., & Sadiq, M. (2023). Impact of climate mitigation technology and natural resource management on climate change in China. Resources Policy, 81. https://doi.org/10.1016/j.resourpol.2023.103367

[5] Ge, L.; Wu, K.; Chang, F.; Zhou, A.; Li, H.; Liu, J., (2021). Deep spatial-temporal fusion network for fine-grained air pollutant concentration prediction. Intell. Data Anal., 25(2): 419–438. https://content.iospress.com/articles/intelligent-data-analysis/ida203208

[6] Geng, Z.; Fan, X.; Lu, X.; Zhang, Y.; Yu, G.; Huang, C.; Wang, Q.; Li, Y.; Ma, W.; Yu, Q.; Wu, L.; Li, H., (2026). FuXi-Air: air quality forecasting based on emission–meteorology–pollutant multimodal machine learning. *npj Clean Air*, 2: 21. https://www.nature.com/articles/s44407-026-00061-w

[7] Gomes, E.; Hossain, I., (2003). Transition from traditional brick manufacturing to more sustainable practices. Energy Sustain. Dev., 7(2): 66–76 . https://www.sciencedirect.com/science/article/pii/S0973082608605545

[8] Haque, S.E.; Shahriar, M.M.; Nahar, N.; Haque, M.S., (2022). Impact of brick kiln emissions on soil quality: A case study of Ashulia brick kiln cluster, Bangladesh. Environ. Chall., 9: 100624. https://www.sciencedirect.com/science/article/pii/S266701002200164X

[9] Hosamane, S.N.; Desai, G.P., (2018). Air pollution modelling from meteorological parameters using artificial neural network. Lect. Notes Comput. Vis. Biomech., 28: 466–475 .https://link.springer.com/chapter/10.1007/978-3-319-71767-8_40

[10] Hu, M.; Liu, B.; Yin, G., (2024). Multi-site and multi-pollutant air quality data modeling. Sustainability, 16(1), 165. 10.3390/su16010165

[11] Intergovernmental Panel on Climate Change (IPCC). (2006). IPCC inventory software user manual.

[12] Intergovernmental Panel on Climate Change (IPCC). (2013). IPCC inventory software user manual version 2.88. https://www.ipcc nggip.iges.or.jp/software/files/IPCCInventorySoftwareUserManualV2_88.pdf

[13] Intergovernmental Panel on Climate Change (IPCC). (2021). Climate Change 2021: The Physical Science Basis. Contribution of Working Group I to the Sixth Assessment Report of the Intergovernmental Panel on Climate Change. Cambridge University Press, Cambridge, UK and New York, USA. https://doi.org/10.1017/9781009157896

[14] Intergovernmental Panel on Climate Change (IPCC). (2022). Climate Change 2022: Mitigation of Climate Change. Contribution of Working Group III to the Sixth Assessment Report of the Intergovernmental Panel on Climate Change. Cambridge University Press. https://doi.org/10.1017/9781009157926

[15] Jadem, A.M.; Jasem, I.M.; Al-Ramahi, F.K.M., (2023). Monitoring pollution and the trend of air quality in brick factories in the Nahrawan region and its impact on Baghdad, using remote sensing data. Ibn Al-Haitham J. Pure Appl. Sci., 36(4): 51–62 (12 pages). https://jih.uobaghdad.edu.iq/index.php/j/article/view/3162

[16] Kazi, Z., Filip, S., & Kazi, L. (2023). Predicting PM2.5, PM10, SO2, NO2, NO and CO Air Pollutant Values with Linear Regression in R Language. Applied Sciences, 13(6), 3617. https://doi.org/10.3390/app13063617

[17] Labaran, Y.H.; Mathur, V.S.; Farouq, M.M., (2021). The carbon footprint of construction industry: A review of direct and indirect emission. J. Sustain. Constr. Mater. Technol., 6(3): 101–115. https://www.jscmt.com

[18] Lawrence, S.; Bhathmanabhan, S., (2026). Harnessing deep learning for air pollution forecasting: trends, techniques, and future prospects. *Artif. Intell. Rev.*, 59: 104. https://link.springer.com/article/10.1007/s10462-026-11496-8

[19] Lee, K.C.; Chen, S.Q., (2026). Transformer encoder for one-step-ahead AQI forecasting using multivariate air-quality monitoring data. Front. Environ. Sci., 14: 1815865. https://www.frontiersin.org/journals/environmental science/articles/10.3389/fenvs.2026.1815865/full

[20] Levermore, G.J. 2008. A review of the IPCC assessment report four, part 1: the IPCC process and greenhouse gas emission trends from buildings worldwide. Building Services Engineering Research and Technology, 29(4), 349-361. https://doi.org/10.1177/0143624408096263

[21] Mai, J.-L., Cai, X.-C., Luo, D.-Y., Zeng, Y., Guan, Y.-F., Gao, W., & Chen, S.-J. (2024). Spatiotemporal variations, sources, and atmospheric transformation potential of volatile organic compounds in an industrial zone based on high-resolution measurements in three plants. Science of the Total Environment, 923, 171352. https://doi.org/10.1016/j.scitotenv.2024.171352

[22] Ministry of Environment, (2024), Ministry of Environment, Baghdad, Iraq.

[23] Ministry of Oil, (2024). Annual Statistical Report 2024. Ministry of Oil, Baghdad, Iraq. Ministry of Oil – Official website

[24] Minx, J.C.; Callaghan, M.; Lamb, W.F.; Garard, J.; Edenhofer, O., (2017). Learning about climate change solutions in the IPCC and beyond. Environ. Sci. Policy, 77: 252–259. https://www.sciencedirect.com/science/article/pii/S1462901117304970

[25] Moradi, H.; Talaiekhozani, A.; Kamyab, H.; Chelliapan, S.; Nadda, A.K., (2024). Development of equations to predict the concentration of air pollutants indicators in Yazd City, Iran. J. Inorg. Organomet. Polym. Mater., 34(1): 38–47. https://link.springer.com/journal/10904

[26] Nasser, M. S., Al-Hassany, J. S., & Al-Jiboori, M. H. (2024). Assessment of air pollution dispersion during wet season: A case study of Rumaila Combined Cycle Power Plant, Basrah, Iraq. Journal of Agrometeorology, 26(4), 411–418. https://doi.org/10.54386/jam.v26i4.2756

[27] Pasic, M., Hadziahmetovic, H., Ahmovic, I., & Pasic, M. (2023). Principal component regression modeling and analysis of PM10 and meteorological parameters in Sarajevo with and without temperature inversion. Sustainability, 15(14). https://doi.org/10.3390/su151411230

[28] Pasic, M.; Bijelonja, I.; Kadric, E.; Bajric, H., (2020). Modeling of nonlinear autoregressive neural network for multi-step ahead air quality prediction. TEM J., 9(3): 852–861. https://www.temjournal.com

[29] Rawat, A.; Sharma, D.K.; Jagannathan, S.K.; Kapahi, M., (2026). Advancing air pollution forecasting: a review of physical, statistical, and machine learning methods. *Environ. Sci. Pollut. Res.*, 33(16): 7373–7398. https://pubmed.ncbi.nlm.nih.gov/42070218/

[30] Amous, S., (2000). Non-carbon dioxide emissions from stationary combustion of fossil fuels. Good practice guidance and uncertainty management in national greenhouse gas inventories. Intergovernmental Panel on Climate Change. https://www.ipcc-nggip.iges.or.jp/public/gp/english/

[31] Seay, B.; Adetona, A.; Sadoff, N.; Sarofim, M.C.; Kolian, M., (2021). Impact of South Asian brick kiln emission mitigation strategies on select pollutants and near-term Arctic temperature responses. Environ. Res. Commun., 3(6): 065001. https://iopscience.iop.org/journal/2515-7620

[32] Shao, Y.; Liu, R.; Huang, S.; Fang, W.; Yang, J.; Liu, M.; Bi, J.; Ma, Z., (2026). Interpretable machine learning for ambient air pollution modeling: A systemic review. *Atmos. Res.*, 336: 108869. https://www.sciencedirect.com/science/article/abs/pii/S016980952600133X

[33] Shatnawi, N.; Abu-Qdais, H., (2021). Assessing and predicting air quality in northern Jordan during the lockdown due to the COVID-19 virus pandemic using artificial neural network. Air Qual. Atmos. Health, 14: 643–652. https://link.springer.com/journal/11869

[34] Shihab, A.S., (2022). Investigating the relationship between air pollutants and meteorology: A canonical correlation analysis. Pol. J. Environ. Stud., 31(6): 5841–5849. https://www.pjoes.com

[35] Song, Z.; Deng, Q.; Ren, Z., (2020). Correlation and principal component regression analysis for studying air quality and meteorological elements in Wuhan, China. Environ. Prog. Sustain. Energy. 39(1): e13218. https://aiche.onlinelibrary.wiley.com/journal/19447447

[36] Statheropoulos, M.; Vassiliadis, N.; Pappa, A., (1998). Principal component and canonical correlation analysis for examining air pollution and meteorological data. Atmos. Environ., 32(6): 1087–1095. https://www.sciencedirect.com/journal/atmospheric-environment

[37] Ukwatta, A.; Mohajerani, A.; Setunge, S.; Eshtiaghi, N., (2018). A study of gas emissions during the firing process from bricks incorporating biosolids. Waste Manage., 74: 413–426. https://www.sciencedirect.com/journal/waste-management

[38] UNEP; GlobalABC, (2024). Global Status Report for Buildings and Construction: Beyond foundations – Mainstreaming sustainable solutions to cut emissions from the buildings sector. United Nations Environment Programme, Nairobi. https://www.unep.org/resources/report/global-status-report-buildings-and-construction

[39] United States Environmental Protection Agency (US EPA), (2024). Criteria Air Pollutants. United States Environmental Protection Agency, Washington, DC, USA. https://www.epa.gov/criteria-air-pollutants

[40] Valdes, H.; Vilches, J.; Felmer, G.; Hurtado, M.; Figueroa, J., (2020). Artisan brick kilns: State-of-the-art and future trends. Sustainability, 12(18): 7526. https://www.mdpi.com/2071-1050/12/18/7526

[41] WeatherSparke. (2024). WeatherSparke website. https://weatherspark.com/h/y/103217/2024/Historical-Weather-during-2024-in-Baghdad-Iraq

[42] Weyant, C.; Kumar, S.; Maithel, S.; Thompson, R.; Baum, E.; Floess, E.; Bond, T., (2016). Brick kiln measurement guidelines: Emissions and energy performance. Climate and Clean Air Coalition; University of Illinois Urbana-Champaign; Greentech Knowledge Solutions Pvt. Ltd. https://www.ccacoalition.org

[43] World Health Organization (WHO), (2021). WHO global air quality guidelines: Particulate matter ($PM_{2.5}$ and PM_{10}), ozone, nitrogen dioxide, sulfur dioxide and carbon monoxide. World Health Organization, Geneva, Switzerland. https://www.who.int/publications/i/item/9789240034228

[44] Xin, D.; Ahmad, M.; Khattak, S.I., (2022). Impact of innovation in climate change mitigation technologies related to chemical industry on carbon dioxide emissions in the United States. J. Clean. Prod., 379: 134746. https://www.sciencedirect.com/journal/journal-of-cleaner-production

[45] Yousefi, M.; Damghani, A.M.; Khoramivafa, M., (2016). Comparison greenhouse gas emissions and global warming potential effect of energy use in different wheat agroecosystems in Iran. Environ. Sci. Pollut. Res., 23: 7390–7397. https://link.springer.com/journal/11356